



Missouri University of Science and Technology
Scholars' Mine

International Conferences on Recent Advances
in Geotechnical Earthquake Engineering and
Soil Dynamics

1991 - Second International Conference on
Recent Advances in Geotechnical Earthquake
Engineering & Soil Dynamics

13 Mar 1991, 1:30 pm - 3:30 pm

Soil-Structure Interaction at the Waterfront

J. M. Ferritto
Naval Civil Engineering Laboratory

Follow this and additional works at: <https://scholarsmine.mst.edu/icrageesd>

 Part of the [Geotechnical Engineering Commons](#)

Recommended Citation

Ferritto, J. M., "Soil-Structure Interaction at the Waterfront" (1991). *International Conferences on Recent Advances in Geotechnical Earthquake Engineering and Soil Dynamics*. 41.
<https://scholarsmine.mst.edu/icrageesd/02icrageesd/session05/41>

This Article - Conference proceedings is brought to you for free and open access by Scholars' Mine. It has been accepted for inclusion in International Conferences on Recent Advances in Geotechnical Earthquake Engineering and Soil Dynamics by an authorized administrator of Scholars' Mine. This work is protected by U. S. Copyright Law. Unauthorized use including reproduction for redistribution requires the permission of the copyright holder. For more information, please contact scholarsmine@mst.edu.



Soil-Structure Interaction at the Waterfront

J.M. Ferritto
Naval Civil Engineering Laboratory

SYNOPSIS: The Navy, forced by its mission to locate at the waterfront, often on loose, saturated cohesionless soils, faces a severe liquefaction threat. Research has been in progress to evaluate the Princeton University Effective Stress Soil Model. This paper discusses that model and presents a validation example study comparing model predictions with a centrifuge experiment.

INTRODUCTION

The Navy has 55 major bases in seismically active regions whose facilities are worth \$25 billion. This includes utilities, roads, bridges, dams, drydocks, piers, and over 14,000 major buildings.

There presently exists a concern to the Navy if major fleet support facilities are damaged. The threat is especially great for West Coast activities where a single earthquake could cause damage to several bases. Many of the buildings at these installations were built without adherence to current seismic standards. The Navy, because of its waterfront mission, must site its facilities on low-lying coastal areas where fine-grained soil conditions are usually marginal and extremely susceptible to large deformation under earthquake loads. High seismicity combined with marginal bearing and saturated soil conditions in areas susceptible to flooding make them especially vulnerable to major damage.

Recent earthquakes, particularly those in Alaska, Japan, and Chile have emphasized the high damage threat the soil liquefaction phenomenon poses to waterfront structures. In the 1960 Chilean earthquake (magnitude 7) quaywalls, sheet piles, and sea walls were damaged by liquefaction of loose, fine, sandy soils. In the 1964 Alaskan earthquake (magnitude 8.4) severe damage to Anchorage, Cordova, and Valdez occurred, including large-scale land slides, as a result of liquefaction. Japanese earthquakes (Niigata, 1964, magnitude 7.3; Miyagi-Ken-Oki, 1978, magnitude 7.4) caused severe waterfront damage to wharfs, bulkheads, quaywalls, piers, and conventional structures. The majority of the damage sustained in waterfront areas was primarily from liquefaction of loose, cohesionless sands (Werner and Hung, 1982).

Each year there is a 5 percent risk of a major earthquake in the Southern California area. Risk to other sites on the West Coast may be only slightly less. Risk also exists to Eastern sites such as Charleston. Each year

the expected loss from seismic damage could approach \$0.5 to 1.0 billion. The conclusions are:

- a. The risk exposure to an earthquake affecting Navy installations is very high.
- b. Given that the earthquake occurs, waterfront facilities are especially vulnerable.

For the above reasons, the Navy has been conducting a research program to develop the technologies necessary to understand the response of structures at the waterfront to the ground motions induced by earthquakes. The large number of unique structures not found in the civilian community makes the task challenging.

Present engineering practice does not consider the presence of the structure in determining the potential for liquefaction. Further, once liquefaction is evaluated, the resulting deformation state is not determined. Clearly this is inadequate to determine the likelihood of liquefaction and the consequences for a major structure. The finite element technique offers the potential for detailed analysis of soil structure problems and has been used extensively. Development of a constitutive model to predict pore pressure and characterize soils in terms of effective stresses (stress on soil grains causing deformation) rather than simple total stress offers the potential capability to analyze complex structures where liquefaction is possible. The finite element method has in recent years been a useful tool in analyzing structures, structures on soil, and soil-structures. An emphasis has been placed on use of nonlinear plasticity soil models to more accurately capture the soil response. Recent Navy research work has focused on effective stress analysis - the ability to not only calculate the soil stress but also to calculate the pore fluid pressure.

An effective stress model can be used for analysis of ocean floor soils and nearshore and offshore structures, for seismic analysis, and for static consolidation. Oscillations in loading, whether from wave action or seismic shaking, produce a dynamic loading that can induce significant increases in pore pressure. The increase in pore pressure can reduce allowable soil capacities and increase deformations by a reduction in effective confining stress. Under extreme conditions flow slides and liquefaction occur. Although liquefaction has been identified as a phenomenon for 20 years, soil mechanics is just beginning to understand the interaction of stress confinement and drainage path, which occurs in the field, such as under a foundation. For example, common engineering practice in the evaluation of seismically-induced soil liquefaction considers level ground conditions away from the structure. Shear stresses from the structure are not considered.

PRINCETON UNIVERSITY EFFECTIVE STRESS MODEL

The Naval Civil Engineering Laboratory (NCEL) undertook a review of available material models. Comparison was made between test data and model predictions (Prevost, et al., 1986). Based on this study, it was concluded that the material model under development at Princeton University by Professor J.H. Prevost was able to predict the behavior of cohesive and cohesionless materials, and that its development was well advanced into the implementation stage in a finite element code (Prevost, 1981). Portions of the development of the research at Princeton University were under Navy sponsorship.

The Princeton University Soil Model represents soil as a two-component system: the soil skeleton and the pore fluid. The hysteretic stress-strain behavior of the soil skeleton is modeled by using the effective-stress elastic-plastic model reported by Prevost (1985). The model is an extension of the simple multi-surface J_2 -plasticity theory and uses conical yield surfaces. The model has been developed to retain the extreme versatility and accuracy of the multi-surface J_2 -theory in describing observed shear nonlinear hysteretic behavior, shear stress-induced anisotropy effects, and to reflect the strong dependency of the shear dilatancy on the effective stress ratio in granular cohesionless soils. The model is applicable to general three-dimensional stress-strain conditions, but its parameters can be derived entirely from the results of conventional triaxial soil tests. The yield function is selected of the following form:

$$f = \frac{3}{2} (\underline{s} - p \underline{g}) \cdot (\underline{s} - p \underline{g}) - m^2 p^2 = 0 \quad (1)$$

where $\underline{s} = \underline{\sigma} - p \underline{\delta} =$ deviatoric stress tensor; $p = 1/3 \text{ tr } \underline{\delta} =$ effective mean normal stress; $\underline{\delta} =$ effective stress tensor; $\underline{g} =$ kinematic deviatoric tensor defining the coordinates of the yield surface center in deviatoric stress subspace; $m =$ material parameter. The yield function plots as a conical yield surface (Drucker-Prager type) in stress space, with its apex at the origin, as shown in Figure 1. Unless $\underline{g} = 0$, the axis of the cone does not coincide with the space diagonal. The cross section of the

yield surface by any deviatoric plane ($p = \text{constant}$) is circular. Its center does not generally coincide with the origin, but is shifted by the amount $p \underline{g}$. This is illustrated in Figure 1 in the principal stress space. The plastic potential is selected such that the deviatoric plastic flow be associative. However, a nonassociative flow rule is used for its dilatational component.

In order to allow for the adjustment of the plastic hardening rule to any kind of experimental data, a collection of nested yield surfaces is used. The yield surfaces are all similar conical surfaces and a purely kinematic hardening rule is adopted. Upon contact, the yield surfaces are translated by the stress point and the direction of translation is selected such that no overlappings of the surfaces can take place. A plastic modulus is associated with each yield surface.

COMPARISON WITH LABORATORY TEST DATA

Soil test data required to develop model material parameters were obtained from a series of drained and undrained triaxial compression and extension tests conducted on a number of sands by universities and private geotechnical firms under NCEL sponsorship (Ferritto, 1983). Cyclic undrained tests and proportional loading tests were also conducted. With detailed soil test data available, NCEL began the task of validating the soil model by using the drained test data to determine model parameters and comparing predicted undrained monotonic and cyclic behavior with actual test data. In general the material model was capable of giving excellent representation of drained test data under a variety of loading conditions using parameters based on drained triaxial compression and extension. The model is capable of giving good agreement with undrained monotonic test data and can track the occurrence of liquefaction in cyclic tests in approximately the same number of cycles. Figures 2, 3, 4, and 5 give typical results.

COMPARISON WITH CENTRIFUGE MODEL

The actual measurement of pore water pressure in the field during an earthquake would serve as the best source of data upon which to validate an effective stress soil model. Unfortunately these data are limited. The centrifuge has been used to study models of undrained soil deposits under seismic type excitation. This can serve as an approximate comparison given that the test data itself is only an indirect measure of field behavior and has errors associated with it.

Storage Tank Test

The centrifuge model consisted of a storage tank placed over a soft foundation strata (Shen, 1985). The tank model was constructed of rolled aluminum plate, which formed the walls. The base consisted of a flexible, rubber membrane to approximate the conditions of a prototype tank's flexible base. A cross section of the model package is presented in Figure 6. Because this is a layered system, which is similar to those found in nature, it is important to correctly capture the effects of all of the layers

on the system response. The displacement traces shown in Figures 7 and 8 show the instantaneous settlement of the sand. Displacement characterization overall is in good agreement while the actual measurements are acceptable. There was some difficulty in the degree of rebound that the numerical model exhibited. The errors here are caused by the difficulty in determining the correct input parameters for the material model as well as soil deposit inconsistencies in placement and uniformity acknowledged by the original investigators. The pore-pressure traces (Figure 9) are in excellent agreement with those measured during the test. Dissipation is represented with excellent accuracy in all cases demonstrating the model's capability in showing three-dimensional consolidation problems.

Soil Columns

The test procedures and test results are reported in Arulanandan (1983). The Monterey sand was pluviated in water in a stacked-ring apparatus. The model test was conducted on a centrifuge at a centrifugal acceleration of 100 gs, and was subjected to a sinusoidal base input acceleration. The corresponding prototype situation was analyzed.

The centrifuge test models free-field conditions by using a stacked-ring device simulating a horizontally layered soil deposit. For the finite element analysis, the soil column is modeled with one row of elements divided into a number of two-dimensional plane elements. Each node was assigned four translational degrees of freedom: two for the soil skeleton and two for the fluid phase (pore-water). The water table is located at the ground surface. No drainage of the pore-fluid is allowed to take place through the rigid bottom boundary and the ground shaking is applied as a horizontal sinusoidal input acceleration at the bottom boundary nodes. As a result of the shaking, excess pore-water pressures build up and partly dissipate in the soil column. The computed pore pressure ratios of 0.69 and 0.85 at two depths compare favorably with 0.74 and 0.86.

Another series of tests were studied using Leighton-Buzzard sand. The test procedures and test results are reported by Lambe (1981). The sand was drained in water, in a stacked-ring apparatus. The model was tested on a centrifuge at a centrifugal acceleration of 35.5 gs, and subjected to a decaying sinusoidal base acceleration. The corresponding prototype situation was analyzed. The water table was located at the ground surface. No drainage of the pore fluid was allowed to take place through the rigid bottom boundary or the side boundaries, and the ground shaking was applied as a horizontal input acceleration at the bottom boundary nodes. Liquefaction occurred in about two cycles both in the centrifuge model and in the computed results.

Footing

A model study from Whitman, et al. (1982) was selected for analysis. The soil was Leighton-Buzzard 120/200 sand. The soil was deposited in a stacked-ring apparatus by pluviating the sand in layers into water and then rodding to achieve the desired density. A brass weight

simulating a footing was placed on top of the saturated sand deposit. The test was conducted in a centrifuge under centrifugal acceleration of 80g. The deposit was then subjected to sinusoidal base acceleration input motion. The soil was discretized by using 240 elements and the brass footing by using two rows of 10 elements each. The brass footing is modeled as a one-phase elastic solid and a static pressure was applied to the top of the footing to achieve the static bearing pressure. The water table was located at the ground surface. No drainage of the pore fluid was allowed to take place through the rigid bottom boundary or through the impermeable sides. A ground shaking was applied as a horizontal sinusoidal input acceleration at the bottom boundary nodes, with a maximum acceleration = 0.17g and a frequency of 1 Hertz for a duration of 10 seconds (10 cycles).

The stacked-ring apparatus controlled the side boundaries in the test. Test boundary conditions were simulated by assigning the same equation number to each nodal degree of freedom on the same horizontal plane for both side boundaries.

An analysis of the computed acceleration time histories shows slight attenuation of base motion at the top of the footing. The computed acceleration time histories at the corners of the footings show rocking motions are imported to the footing. Settlement beneath the footing increases continuously and almost linearly while shaking occurs. Further, no additional significant settlements are computed to occur after the shaking stops as noted in the test. As observed in the test, in the "free-field" away from the structure, the pore-water pressure rises quickly. Directly under the structure, the pore-pressure increase is slower and always remains lower than the pore-pressure in the free-field at the same elevation. Immediately following shaking, the excess pore-pressures dissipate rapidly and reach their steady state conditions 5 seconds after the end of the shaking. This is further illustrated in Figure 6 which shows time histories for the vertical effective stress and excess pore-water pressures. Also shown in Figure 10 is a comparison of computed pore-pressure in comparison with the measured values. The computer simulation gives qualitatively good agreement showing liquefaction to occur in the same regions as observed in the test and also gives comparable pore-pressure ratios.

TAIWAN TEST SITE

The Electric Power Research Institute and the Taiwan Power Company designed and constructed a 1/4 scale and 1/12 scale reinforced concrete containment structure in Lotung, Taiwan. This site was selected for its high seismic activity. Under joint National Science Foundation and NCEL sponsorship, the University of California, Davis instrumented the site with piezometers to record pore pressure buildup during an earthquake.

The test site is located in the southern part of the Lanyang Plain of Northeastern Taiwan. The Lanyang River is located approximately 2 miles north of the test site. The plain is

covered almost completely by alluvium. A detailed site exploration was completed including geophysical seismic up-hole and cross-hole tests, and a refraction survey. An Artesian pressure condition was noted at the site with a water table 2 to 3 feet below ground level. The potential for liquefaction was estimated to occur with acceleration levels as low as 0.06 to 0.20g.

A number of earthquakes in the magnitude range of 5 to 7 have been observed and recorded at the site. Two events at magnitude 6.2 in July 1986 and a magnitude 7.0 in November 1986 are being studied using the Effective Stress Soil Model.

REFERENCES

- Arulanandan, K., A. Anandarajah, and A. Abghari (1983), "Centrifugal Modeling of Soil Liquefaction Susceptibility," *Journal Geotechnical Engineering, American Society of Civil Engineers*, vol 109, no. 3, pp 281-300.
- Ferritto, J.M. et al. (1983), "Utilization of the Prevost Soil Model for Soil-Structure Problems," *Naval Civil Engineering Laboratory, Technical Memorandum M-51-83-09*, Port Hueneme, CA.
- Lambe, P.C. (1981), "Dynamic Centrifugal Modeling of a Horizontal Sand Stratum," *Sc. D. Thesis*, MIT, Cambridge, MA.
- Prevost J.H., J. Ferritto, and R. Slyh (1986), "Evaluation and Validation of the Princeton University Stress Model," *Naval Civil Engineering Laboratory, Technical Report R-919*, Port Hueneme, CA,
- Prevost, J.H. (1981), "DYNAFLOW: A Nonlinear Transient Finite Element Analysis Program," *Princeton University, Department of Civil Engineering*, Princeton, NJ.
- Prevost, J.H. (1985), "A Simple Plasticity Theory for Frictional Cohesionless Soils," *International Journal of Soil Dynamics and Earthquakes Engineering*, vol 4 (1).
- Shen, et al. (1985), "Centrifuge Consolidation Study for Purpose of Plasticity Theory Validation," *University of California, Davis, CA*.
- Werner, S.D. and Hung (1982), "Seismic Response of Port and Harbor Facilities," *Azabian Associates, Report No. R-8122-5395*.
- Whitman, R.V. and P.C. Lambe (1982), "Liquefaction: Consequences for a Structure," *Proceedings of the Soil Dynamics and Earthquake Engineering Conference*, Southampton, U.K.

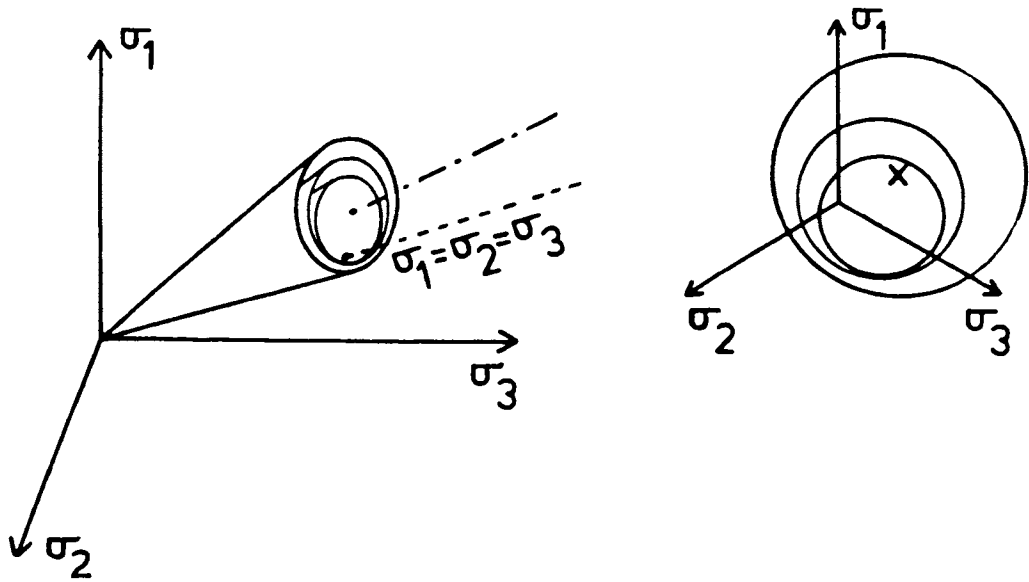


Figure 1. Yield surfaces in principal stress space.

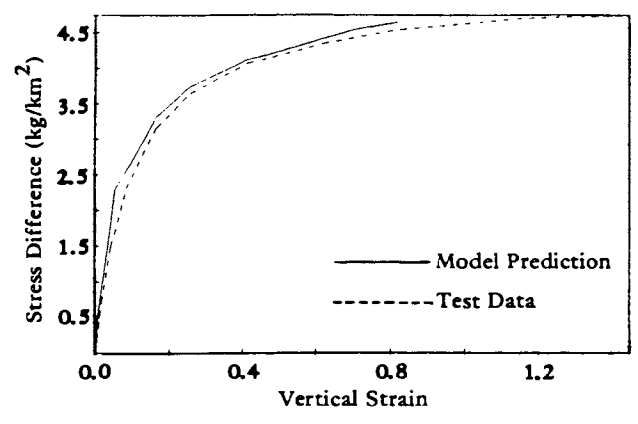


Figure 2. Drained compression test.

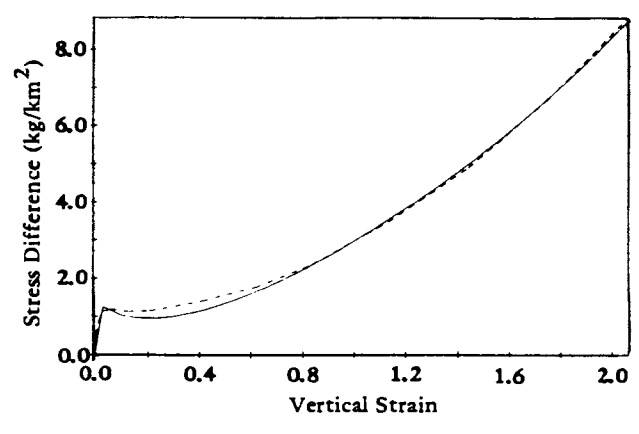


Figure 3. Undrained compression test.

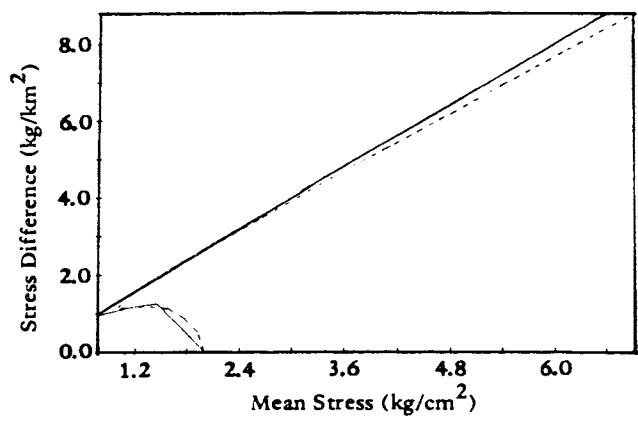


Figure 4. Undrained stress path.

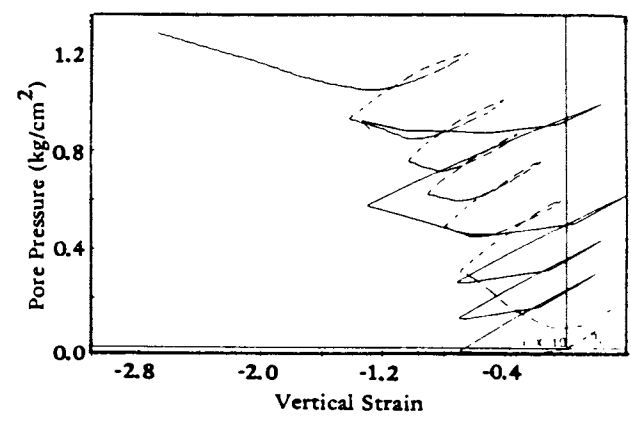


Figure 5. Cyclic test results.

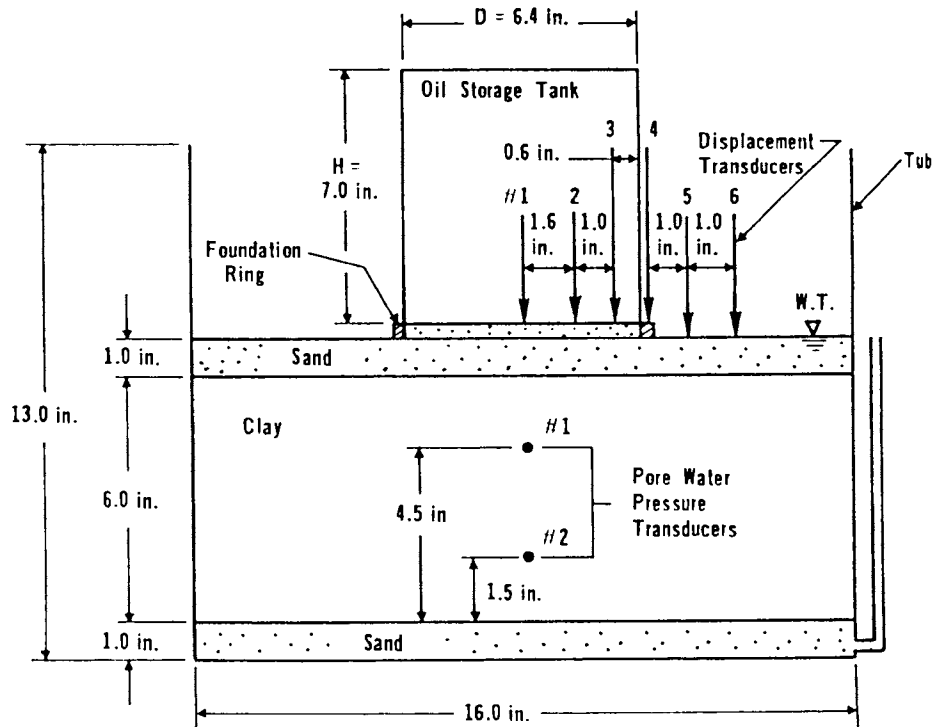


Figure 6. Model tank package.

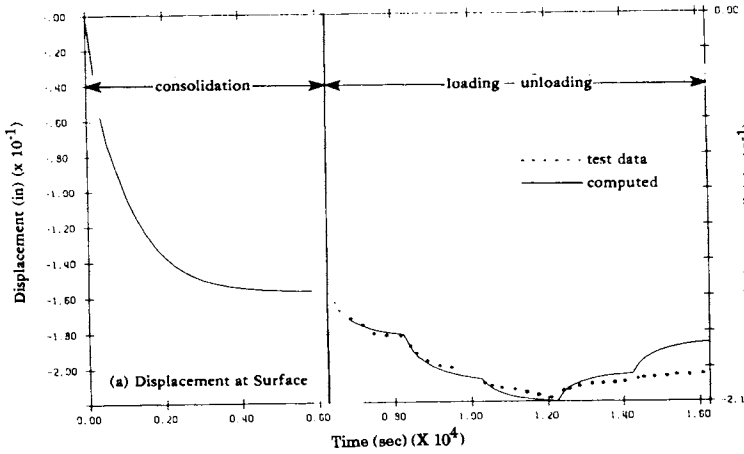


Figure 7. Vertical displacement along centerline.

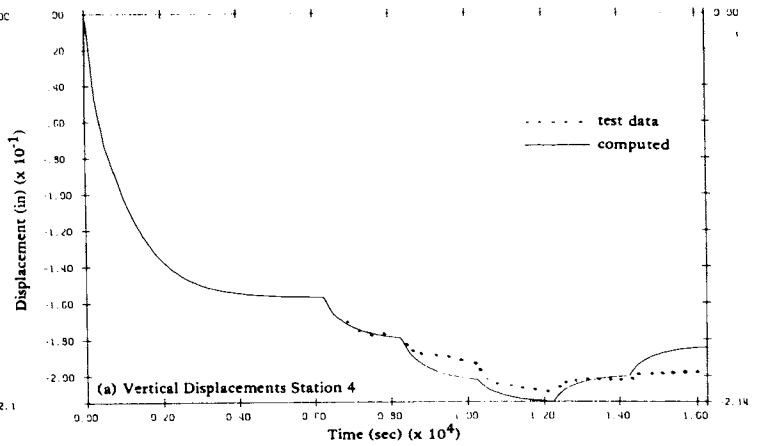


Figure 8. Free-field displacements.

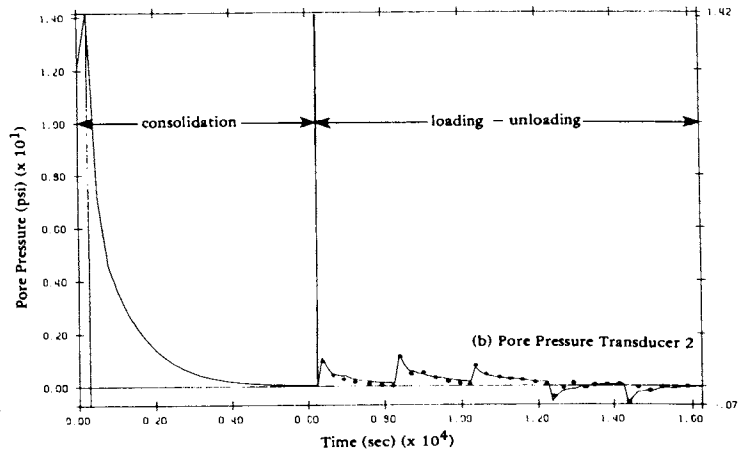
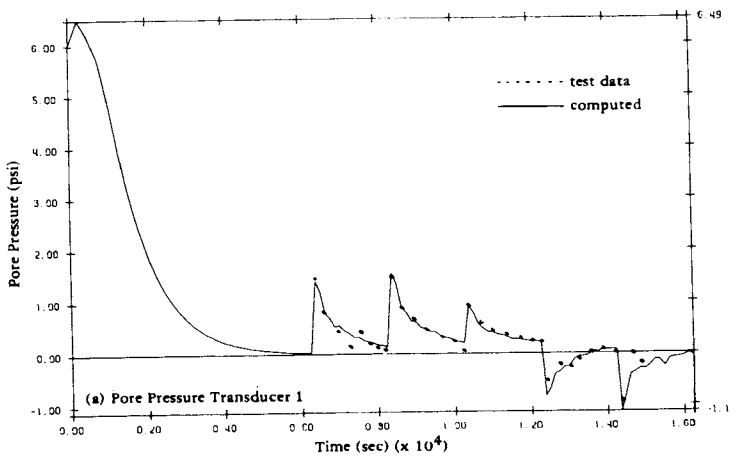
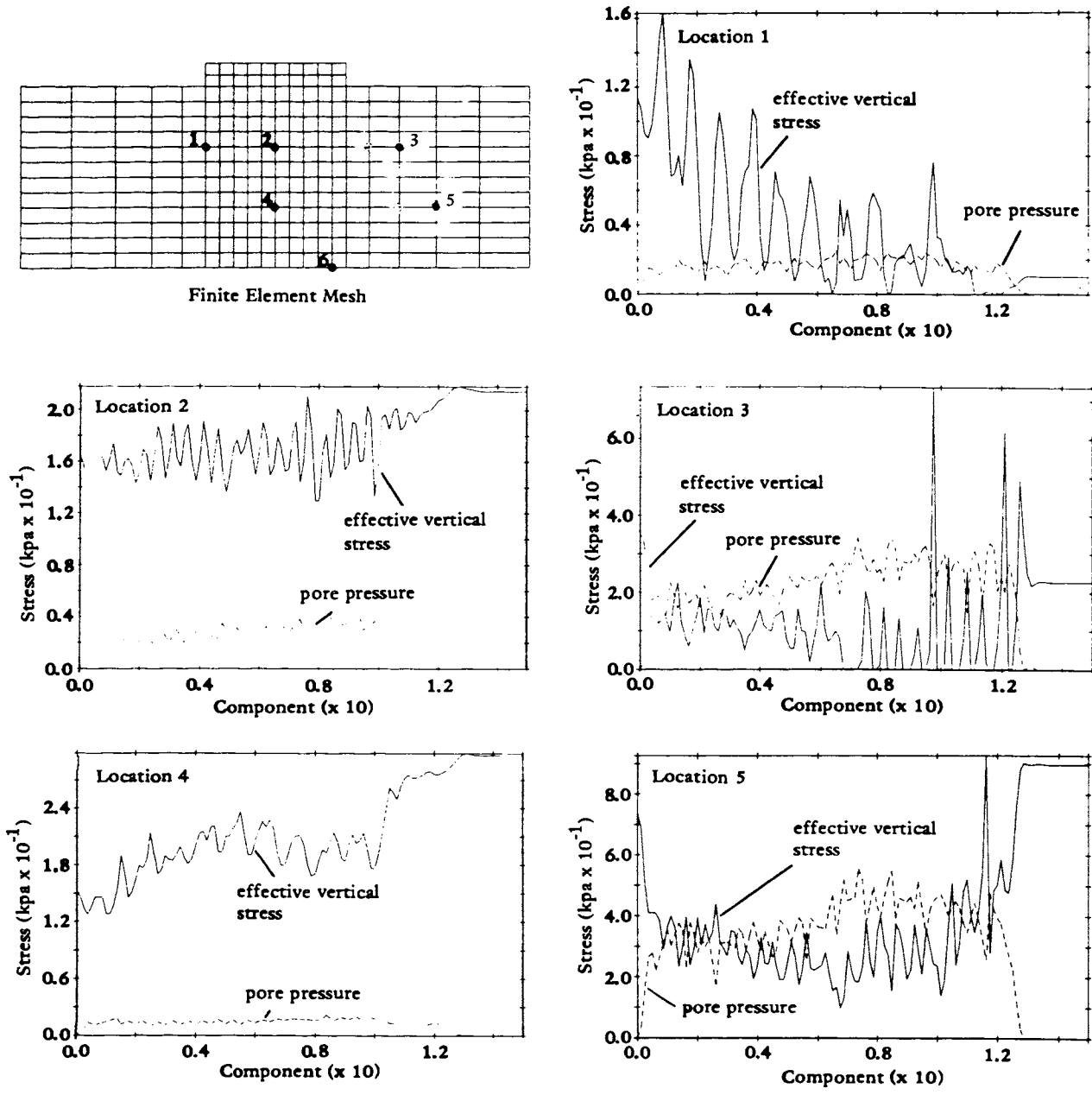


Figure 9. Pore-pressure traces.



Peak Pore Pressure (kpa)

Location	Computer	Measured
1	20	20
2	30	30
3	30	25
4	15	12
5	50	65
6	40	60

Figure 10. Simulated footing results.